

DEEP INFRARED ZAMS FITS TO BENCHMARK OPEN CLUSTERS HOSTING δ SCUTI STARS

Daniel J. Majaess^{1,2}, David G. Turner^{1,2}, David J. Lane^{1,2}, Tom Krajci^{3,4}

¹ *Saint Mary's University, Halifax, Nova Scotia, Canada*

² *The Abbey Ridge Observatory, Stillwater Lake, Nova Scotia, Canada*

³ *Astrokolkhoz Telescope Facility, Cloudcroft, New Mexico, USA*

⁴ *American Association of Variable Star Observers, Cambridge, MA, USA*

dmajaess@cygnus.smu.ca

ABSTRACT

This research aims to secure precise distances for cluster δ Scutis in order to investigate their properties via a *VI* Wesenheit framework. Deep *JHK_s* colour-colour and ZAMS relations derived from $\simeq 700$ unreddened stars featuring 2MASS photometry and precise Hipparcos parallaxes ($d \lesssim 25$ pc) are applied to establish distances to several benchmark open clusters that host δ Scutis: Hyades, Pleiades, Praesepe, α Persei, and M67 ($d = 47 \pm 2, 138 \pm 6, 183 \pm 8, 171 \pm 8, 815 \pm 40$ pc). That analysis provided constraints on the δ Sct sample's absolute Wesenheit magnitudes ($W_{VI,0}$), evolutionary status, and pulsation modes (order, n). The reliability of *JHK_s* established cluster parameters is demonstrated via a comparison with van Leeuwen (2009a) revised Hipparcos results. Distances for 7 of 9 nearby ($d \leq 250$ pc) clusters agree, and the discrepant cases (Pleiades & Blanco 1) are unrelated to (insignificant) $T_e - (J - K_s)$ variations with cluster age or iron abundance. *JHK_s* photometry is tabulated for $\simeq 3 \times 10^3$ probable cluster members on the basis of proper motions (NOMAD). The deep *JHK_s* photometry extends into the low mass regime ($\simeq 0.4M_\odot$) and ensures precise ($\leq 5\%$) ZAMS fits. Pulsation modes inferred for the cluster δ Scutis from *VI* Wesenheit and independent analyses are comparable ($\pm n$), and the methods are consistent in identifying higher order pulsators. Most small-amplitude cluster δ Scutis lie on *VI* Wesenheit loci characterizing $n \geq 1$ pulsators. A distance established to NGC 1817 from δ Scutis ($d \simeq 1.7$ kpc) via a universal *VI* Wesenheit template agrees with estimates in the literature, assuming the variables delineate the $n \geq 1$ boundary. Small statistics in tandem with other factors presently encumber the use of mmag δ Scutis as viable distance indicators to intermediate-age open clusters, yet a *VI* Wesenheit approach is a pertinent means for studying δ Scutis in harmony with other methods.

Subject headings: δ Scuti variables — Hertzsprung-Russell and colour-magnitude diagrams — infrared: stars — open clusters and associations: general.

1. INTRODUCTION

δ Sct variables are unique among standard candles of the classical instability strip for permitting the determination of distances to population I and II environments from a single *VI* Wesenheit calibration. SX Phe and other metal-poor population II δ Scutis lie toward the short-period extension of the Wesenheit ridge characterizing population I δ Scutis (Fig. 3 in Majaess et al. 2010, see also Petersen & Høg 1998). That presents an opportunity to bridge and strengthen the distance scales tied to globular clusters, open clusters, nearby galaxies, and the Galactic center where such variables are observed (McNamara et al. 2000, 2007; Poleski et al. 2010; Majaess et al. 2010). To that end the present research examines δ Sct calibrators associated with benchmark open clusters via a *VI* Wesenheit framework, an analysis which relies on the establishment of precise cluster distances and multiband photometry (*VIJHK_s*).

In this study, infrared colour-colour and ZAMS relations are constructed from unreddened stars in close proximity to the Sun with precise Hipparcos parallaxes (§2). The relations are subsequently employed to establish parameters for five benchmark open clusters which host δ Scutis, namely the Hyades, Pleiades, Praesepe, α Persei, and M67 (§2). Cluster membership provides constraints on the absolute Wesenheit magnitudes ($W_{VI,0}$), evolutionary status, and pulsation modes (order, n) for the δ Scutis (§3). An independent determination of the cluster parameters is pursued since the objects form the foundation of the open cluster scale and yet their distances are uncertain. Most notably the Hipparcos distance to stars in the Pleiades is $d = 120.2 \pm 1.9$ pc (van Leeuwen 2009a), whereas HST observations imply $d = 134.6 \pm 3.1$ pc (Soderblom et al. 2005). Likewise, four Hipparcos-based distances cited in the literature for α Persei disagree (Table 1). In §3, a Wesenheit analysis

(VI) is shown to be a viable means for investigating δ Scutis. Lastly, the distance to NGC 1817 is evaluated via a universal Wesenheit template using new VI photometry acquired from the Abbey Ridge Observatory (ARO, Lane 2007; Turner et al. 2009a) for the cluster's numerous δ Scutis (§3.4).

2. JHK_s INTRINSIC RELATIONS

Intrinsic colour-colour and ZAMS relations are derived from JHK_s photometry for A, F, G, K, and M-type stars that feature precise parallaxes ($d \lesssim 25$ pc). The infrared photometry and parallaxes are provided via the 2MASS and Hipparcos surveys (Perryman & ESA 1997; Cutri et al. 2003; Skrutskie et al. 2006). 2MASS photometry may be saturated for nearby stars, yet reliable data are available for fainter stars of late spectral type. The photometric uncertainties thus increase for brighter early-type stars (Fig. 1), which are already undersampled owing to the nature of the initial mass function. Spurious data deviating from the evident intrinsic functions were excluded.

$M_J/(J - H)_0$ and $M_J/(J - K_s)_0$ colour-magnitude diagrams for the calibration are presented in Fig. 1 (red dots). The latter passband combination exhibits smaller uncertainties. $(J - H)_0/(H - K_s)_0$ and $(J - K_s)_0/(H - K_s)_0$ colour-colour diagrams are likewise shown in Fig. 1 (red dots). Infrared relations offer advantages over those founded on UBV photometry owing to the mitigated impact of chemical composition (§2.1, Fig. 3), differential reddening, and total extinction.

Colour-magnitude and colour-colour diagrams were assembled for the target clusters by obtaining 2MASS photometry for members on the basis of proper motions (Figs. 1, 2). The Naval Observatory Merged Astrometric Dataset (NOMAD, Zacharias et al. 2004) features proper motion data for the fields inspected. JHK_s photometry for $\sim 3 \times 10^3$ probable clusters members were tabulated, and the list includes several previously unidentified members. That sample shall be made available online via the *Centre de Données astronomiques de Strasbourg*. Photometry for the brighter stars may be saturated, as noted earlier, while lower mass members are catalogued despite being near the faint-limit of the 2MASS survey. High-precision multi-epoch JHK_s data for M67 is available from Nikolaev et al. (2000, see also Sarajedini et al. 2009).

Reddenings for the target clusters were secured by shifting the intrinsic colour-colour relations to the observed data (Fig. 1). JHK_s extinction laws were adopted from Bonatto et al. (2008) and references therein. The distance to a cluster follows by matching the ZAMS to the observed data for the reddening established by the intrinsic colour-colour relations. Precise results were obtained because the trends for late-type stars in JHK_s colour-magnitude and colour-colour diagrams provide excellent anchor points for fitting ZAMS

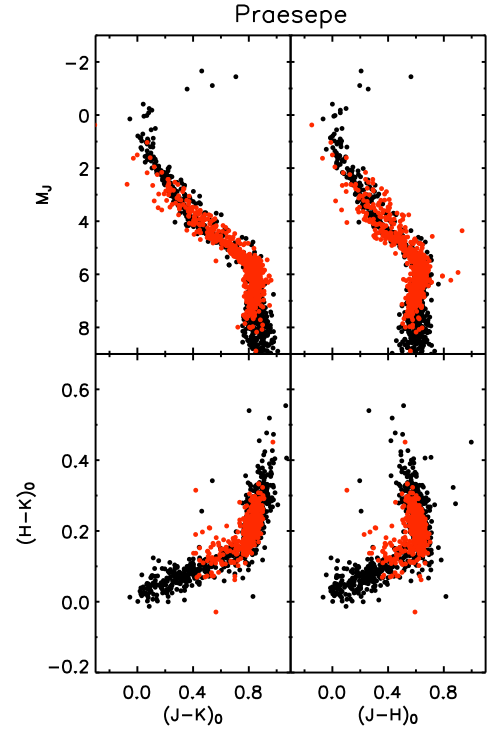


Fig. 1.— Deep 2MASS JHK_s colour-magnitude and colour-colour diagrams for the calibration (red dots) and Praesepe star cluster (black dots). Likely members of the Praesepe were selected on the basis of proper motions (NOMAD). The resulting parameters are $E(J - K_s) = 0.025 \pm 0.015$ and $d = 183 \pm 8$ pc.

and intrinsic relations (Figs. 1, 2). $J - K_s$ and $J - H$ were observed to remain nearly constant and become bluer with increasing magnitude ($M_J \gtrsim 6$) for low mass main-sequence stars beginning near spectral type M (Figs. 1, 2, see also Sarajedini et al. 2009 and references therein), and a sizable separation exists between main-sequence and evolved M-type stars in the JHK_s colour-colour diagram (see also Straižys & Laugalys 2009). Turner (2010b) developed intrinsic JHK_s functions to describe early-type stars ($\lesssim K0$) via an alternate approach.

Distances obtained for the benchmark clusters examined are summarized in Table 1.

2.1. AGE AND METALLICITY DEPENDENCIES

The JHK_s distances agree with van Leeuwen (2009a) Hipparcos results for 7 of 9 star clusters within 250 pc (Table 1). The distance determined here to the Pleiades favours the HST estimate rather than that established by Hipparcos (Table 1).¹ Soderblom et al. (2005) (& others) argue that the Hipparcos distance to the Pleiades is erroneous. Conversely, the reliability of the ZAMS dis-

¹The HST and Hipparcos Pleiades surveys lack overlap, and the former exhibits comparatively smaller statistics.

Table 1: Distances to Benchmark Open Clusters

Cluster	HIP (M97)	HIP (R99)	HIP (V99)	HIP (V09)	<i>JHK_s</i>	HST
M67	815 ± 40 pc	...
Hyades	46.45 ± 0.50 pc	47 ± 2 pc	48.3 ± 2.0 pc
Praesepe	177.0 ± 10.3 pc	180.5 ± 10.7 pc	180 pc	181.6 ± 6.0 pc	183 ± 8 pc	...
Pleiades	116.3 ± 3.3 pc	118.2 ± 3.2 pc	125 pc	120.2 ± 1.9 pc	138 ± 6 pc	134.6 ± 3.1 pc
α Persei	184.2 ± 7.8 pc	190.5 ± 7.2 pc	170 pc	172.4 ± 2.7 pc	171 ± 8 pc	...
Coma Ber*	88.2 ± 1.7 pc	87.0 ± 1.6 pc	86 pc	86.7 ± 0.9 pc	85 ± 6 pc	...
Blanco 1	252.5 ± 31.1 pc	263 ± 31 pc	190 pc	207 ± 12 pc	240 ± 10 pc	...
IC 2391*	147.5 ± 5.4 pc	146.0 ± 4.7 pc	140 pc	144.9 ± 2.5 pc	134 ± 13 pc	...
IC 2602*	146.8 ± 4.7 pc	152 ± 3.7 pc	155 pc	148.6 ± 2.0 pc	147 ± 14 pc	...
NGC 2451*	...	188.7 ± 6.8 pc	220 pc	183.5 ± 3.7 pc	189 ± 15 pc	...

Notes: Hipparcos (HIP) distances from Mermilliod et al. (1997, M97), Robichon et al. (1999a, R99), van Leeuwen (1999, V99), and van Leeuwen (2009a, V09). HST distances to the Hyades and Pleiades from van Altena et al. (1997) and Soderblom et al. (2005). *JHK_s* results from this study. Clusters highlighted by an asterisk were more difficult to assess (*JHK_s*). Iron abundances and age estimates for the clusters are tabulated in Mermilliod et al. (1997) and van Leeuwen (1999).

tance to the Pleiades has been questioned owing to the possible neglect of colour- T_e variations with stellar age and chemical composition. The matter is now investigated.

An age-luminosity effect has been proposed as a possible source for the disagreement between the ZAMS and Hipparcos distance to the Pleiades. That hypothesis is not supported by the infrared distances established here. The Hyades, Praesepe, and α Persei clusters bracket the discrepant cases of the Pleiades and Blanco 1 in age (Table 1). *JHK_s* and van Leeuwen (2009a) Hipparcos distances to the former clusters are in broad agreement (Table 1). The comparatively nearby ($d \leq 250$ pc) open clusters IC 2602, NGC 2451, IC 2391, and Coma Ber were investigated to bolster the case, but proved more difficult to assess. The Hipparcos distance to the Pleiades implies that the cluster’s ZAMS is a sizable $\simeq 0^{\text{m}}.4$ below the faintest calibration stars (Fig. 1, where the photometric uncertainties are minimized, $M_J/(J - K_s)_0$). The Hipparcos zero-point for the Pleiades is inconsistent with a $M_J/(J - K_s)_0$ ZAMS calibration (Fig. 1) which features stars of differing age, chemical composition, and peculiarities.

The clusters in Table 1 exhibiting discrepant distances are not correlated with iron abundance. That supports Alonso et al. (1996) and Percival et al. (2005) assertion that $J - K_s$ is relatively insensitive to metallicity over the baseline examined. Percival et al. (2005) suggested that $J - K_s$ may exhibit a marginal dependence on metallicity, but cautioned that the errors are sizable and the correlation coefficient is consistent with zero. The impact of a marginal $T_e - [\text{Fe}/\text{H}] - (J - K_s)$ dependence appears insignificant since stars belonging to the clusters examined display near solar iron abundances (Mermilliod et al. 1997; van Leeuwen 1999, their Table 1). 270 calibration stars (Fig. 1) featured in

Soubiran et al. (2010) PASTEL catalogue of stellar atmospheric parameters exhibit a peak distribution near $[\text{Fe}/\text{H}] \simeq -0.05$, which is analogous to or inappreciably less than members of the Pleiades ($[\text{Fe}/\text{H}] = -0.039 \pm 0.014, +0.03 \pm 0.05, +0.06 \pm 0.01$, Taylor 2008; Soderblom et al. 2009; Paunzen et al. 2010). Colours for calibrating stars (Fig. 1) in PASTEL were plotted as a function of effective temperature and metallicity (Fig. 3, optical photometry from Mermilliod 1991). $B - V$ and $U - B$ colour indices appear sensitive to iron abundance whereby metal-rich stars are hotter at a given colour (Fig. 3), as noted previously (Turner 1979, and references therein). Conversely, $J - K_s$ appears comparatively insensitive to iron abundance over the restricted baseline examined (Fig. 3). Yet the results should be interpreted cautiously and in tandem with the other evidence presented given the semi-empirical nature of that analysis (T_e and $[\text{Fe}/\text{H}]$ are model dependent).

The clusters exhibit a similar ZAMS morphology in the infrared ($M_J/(J - K_s)_0$, Figs. 1, 2). The Hyades, Praesepe, Pleiades, and M67 ZAMS (un-evolved members) are nearly indistinguishable (Fig. 2). Stauffer et al. (2003) likewise noted that the Praesepe and Pleiades cluster share a ZAMS ($M_v/(V - I)_0$) that is essentially coincident throughout. By contrast, the apparent sensitivity of optical photometry to metallicity may explain (in part) certain anomalies which distinguish individual clusters in optical colour-magnitude and colour-colour diagrams (Fig. 3, see also Turner 1979; Mermilliod et al. 1997; Stauffer et al. 2003; van Leeuwen 2009a). Compounded uncertainties prevent a direct assessment of the infrared colour-colour function’s universality ($(J - K_s)_0/(H - K_s)_0$). Minimizing the uncertainties associated with the *JHK_s* photometry and extending the restricted temperature baseline are desirable. Fainter *JHK_s* observations could be acquired from l’Observatoire Mont-Mégantique or the

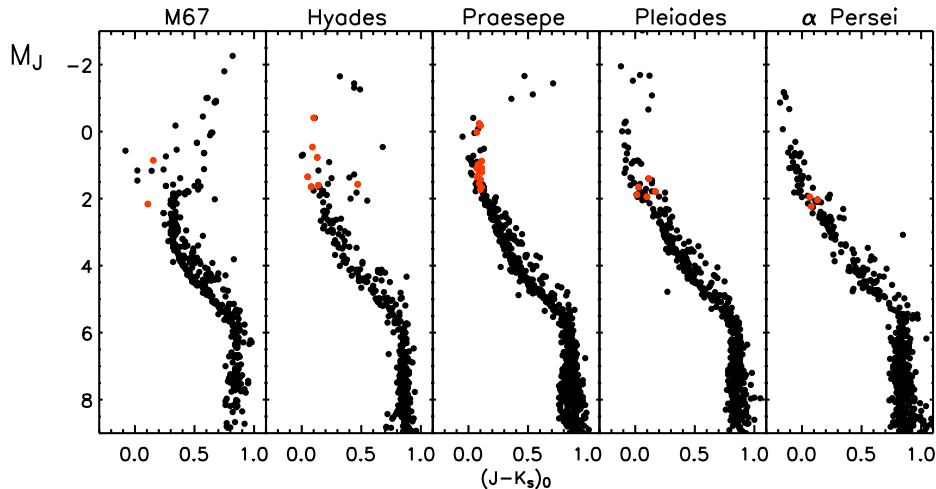


Fig. 2.— Deep 2MASS JHK_s colour-magnitude diagrams for M67, Hyades, Praesepe, Pleiades, and α Persei star clusters. The clusters feature a common ZAMS morphology in the infrared. The δ Scutis examined in §3 (red dots) may be evolved (Hyades/Praesepe), blue stragglers (M67), or occupy the binary / rapid rotator sequence (Pleiades).

forthcoming VVV survey (Artigau et al. 2009, 2010; Minniti et al. 2010), whereas brighter stars could be observed as part of the AAVSO’s IR photoelectric photometry program (Henden 2002; Templeton 2009).

In sum, neither variations in iron abundance or stellar age readily explain the discrepancies between the JHK_s ZAMS and Hipparcos distances (Table 1). It is emphasized that the problematic cases (the Pleiades & Blanco 1) constitute the minority (Table 1). Note that the four published Hipparcos distances to Blanco 1 exhibit a sizable 20% spread (Table 1, see also α Persei). Further research is needed, and the reader should likewise consider the interpretations of Mermilliod et al. (1997), Robichon et al. (1999b), Soderblom et al. (2005), and van Leeuwen (2009a,b).

3. CLUSTER δ SCUTIS

3.1. VI PHOTOMETRY

The cluster δ Scutis examined are summarized in Table 4, along with references for their VI photometry. Certain sources feature I -band photometry not standardized to the Cousins system (e.g., Mendoza 1967). Additional observations for the δ Scutis were obtained via the AAVSO’s Bright Star Monitor (BSM)² and the Naval Observatory’s Flagstaff Station (NOFS) (Table 2). The BSM features an SBIG ST8XME CCD (fov: $127' \times 84'$) mounted upon a 6-cm wide-field telescope located at the Astrokolkozh telescope facility near Cloudcroft, New Mexico. The AAVSO observations are tied to Landolt (1983, 1992) photometric standards according to precepts outlined in Henden & Kaitchuck (1990) (see also Henden & Munari 2008).

VI photometry is used since LMC and Galactic δ Scutis follow VI Wesenheit relations which vary as a function of the pulsation order n (Fig. 4, Poleski et al. 2010; Majaess et al. 2010), thereby enabling constraints on that parameter for target δ Scutis at common or known distances (see §3.3). Furthermore, the author has advocated that RR Lyrae variables and Cepheids—which partly form the basis for the calibration used in §3.2—obey VI Wesenheit and period-colour relations which are comparatively insensitive to metallicity (Majaess et al. 2008, 2009a,b; Majaess 2009, 2010a,b, see also Bono & Marconi 1999; Udalski et al. 2001; Bono 2003; Pietrzyński et al. 2004; Bono et al. 2008). For example, Majaess (2010b) reaffirmed that the slope of the VI Wesenheit function for Milky Way Classical Cepheids (Benedict et al. 2007; Turner 2010a) characterizes classical Cepheids in the LMC, NGC 6822, SMC, and IC 1613 (see Fig. 2 in Majaess 2010b). Classical Cepheids in the aforementioned galaxies exhibit precise ground-based photometry, span a sizable abundance baseline, and adhere to a common VI Wesenheit slope to within the uncertainties ($\alpha = -3.34 \pm 0.08(2\sigma)$, $\Delta[\text{Fe}/\text{H}] \simeq 1$). More importantly, Majaess (2010b) noted that a negligible distance offset exists between OGLE classical Cepheids and RR Lyrae variables in the LMC, SMC, and IC 1613 as established via a VI Wesenheit function, thereby precluding a dependence on metallicity. Admittedly, the impact of a reputed metallicity effect is actively debated in the literature (Smith 2004; Romaniello et al. 2008; Catelan 2009, and references therein). By contrast there appears to be a consensus that relations which rely on BV photometry are sensitive to variations in chemical abundance, and a significant break in the period-magnitude relation is apparent (Majaess et al. 2008, 2009b and references therein).

²<http://www.aavso.org/aavsonet>

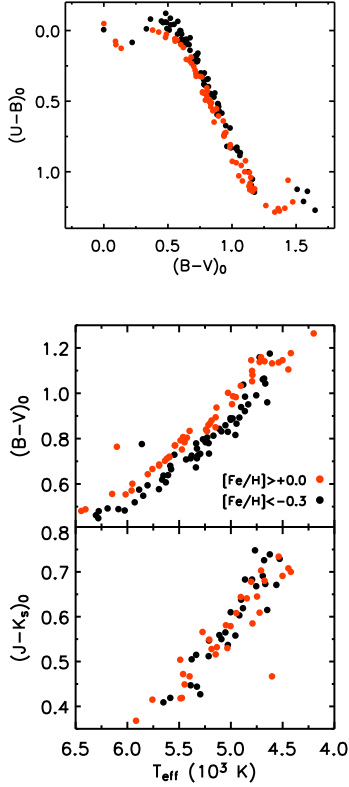


Fig. 3.— Semi-empirical colour- T_{eff} - $[\text{Fe}/\text{H}]$ correlation for calibration stars (Fig. 1) featured in PASTEL. Red and black dots indicate metal-rich and metal-poor stars accordingly. $B-V$ and $U-B$ colour indices appear sensitive to metallicity, whereas $J-K_s$ is comparatively unaffected by changes in iron abundance (see text).

Table 2: New Photometry for Cluster δ Scutis

Star	Cluster	CMD position (Fig. 2)	V	$V-I_c$
EX Cnc	M67	BS	10.90	0.30
EW Cnc	M67	BS	12.24	0.30
HD 23156	Pleiades	MS	8.23	0.28
HD 23194	Pleiades	MS	8.08	0.20
HD 23567	Pleiades	MS	8.29	0.41
HD 23607	Pleiades	MS	8.25	0.27
HD 23628	Pleiades	MS,BR	7.69	0.24
HD 23643	Pleiades	MS,BR	7.79	0.16

Notes: magnitudes are means of observations acquired from the AAVSO’s BSM, NOFS, TASS (Droege et al. 2006), and Mendoza (1967). The identifiers are as follows: stars occupying the blue straggler region (BS), binary / rapid rotator sequence (BR), and main-sequence (MS) of the colour-magnitude diagram (Fig. 2).

The results are consistent (in part) with the findings of §2.1, however, a direct comparison is not valid.

3.2. WESENHEIT MAGNITUDES

A Wesenheit diagram segregates variables into their distinct classes (Fig. 4). Wesenheit magnitudes for the cluster δ Scutis were computed as follows:

$$W_{VI,0} = \langle V \rangle - R_{VI}(\langle V \rangle - \langle I \rangle) - \mu_0 \quad (1)$$

μ_0 is the distance modulus from Table 1 and $R_{VI} = 2.55$ is the canonical extinction law, although there are concerns with adopting a colour-independent extinction law. VI Wesenheit magnitudes are reddening-free and comparatively insensitive to chemical composition and the width of the instability strip. The Wesenheit function is defined and discussed in the following references: Madore (1982), Opolski (1983, 1988), Madore & Freedman (1991, 2009), Kovács & Jurcsik (1997), Kovács & Walker (2001), Di Criscienzo et al. (2004, 2007), and Turner (2010a).

Cluster δ Scutis in Tables 3 and 4 are plotted on a universal VI Wesenheit template (Fig. 4, see also Majaess et al. 2010). 30 variables with distances measured by geometric means formed the calibration (Majaess et al. 2010, their Table 1). The sample consisted of 8 SX Phe and δ Sct variables (HIP, van Leeuwen 2007), 4 RR Lyrae variables (HIP and HST, Benedict et al. 2002b; van Leeuwen 2007), 2 Type II Cepheids (HIP, van Leeuwen 2007), and 10 classical Cepheids (HST, Benedict et al. 2002a, 2007). That sample was supplemented by 6 Type II Cepheids detected by Macri et al. (2006) in their comprehensive survey of the galaxy M106 (Majaess et al. 2009b), which features a precise geometric-based distance estimate (VLBA, Herrnstein et al. 1999). Type II Cepheids within the inner region of M106 were not incorporated into the calibration because of the likelihood of photometric contamination via crowding and blending (Majaess et al. 2009b, 2010; Majaess 2010b, see also Stanek & Udalski 1999; Mochejska et al. 2001; Macri et al. 2006; Vilardell et al. 2007; Smith et al. 2007). The stars employed were observed in the outer regions of M106 where the stellar density and surface brightness are diminished by comparison. Admittedly, it is perhaps ironic that stars 7.2 Mpc distant may be enlisted as calibrators owing to an absence of precise parallaxes for nearby objects. Additional observations of new variables in M106 are forthcoming (Macri & Riess 2009).

LMC variables catalogued by OGLE, including the latest sample of δ Scutis (Poleski et al. 2010), were added to the Wesenheit template (Fig. 4, OGLE data: Udalski et al. 1999; Soszyński et al. 2002, 2003, 2008,b, 2009, see also Udalski 2009). The LMC data were calibrated with a distance established via the geometric-anchored universal Wesenheit template ($\mu_0 = 18.43 \pm 0.03(\sigma_{\bar{x}})$, Majaess et al. 2010). That distance agrees with a mean derived from 300+ results tabulated for the LMC at the NASA/IPAC Extragalactic Database

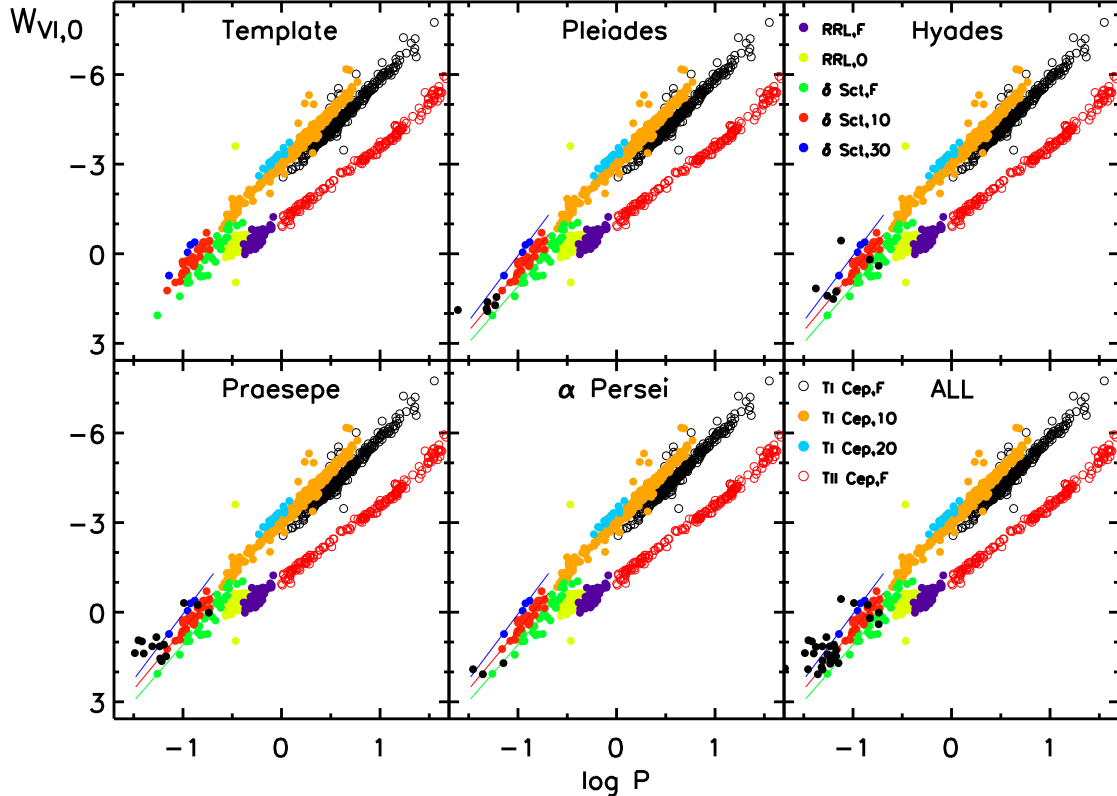


Fig. 4.— A calibrated universal VI Wesenheit template constructed from data presented in Majaess et al. (2010) and the latest OGLE III observations (e.g., Poleski et al. 2010). The cluster δ Scutis are displayed as black dots. Wesenheit magnitudes were computed via Eqn. 1 using the JHK_s established cluster distances and VI photometry highlighted in Tables 1 & 4 accordingly. First-order constraints on the inferred pulsation modes (n) are listed in Tables 3 & 4.

(NED) (Madore & Steer 2007; Steer & Madore 2010,^{3,4} see also Fig. 2 in Freedman & Madore 2010). Adding Turner (2010a) list of classical Cepheids in Galactic clusters to the universal VI Wesenheit calibration yields the same LMC distance with reduced uncertainties.

The universal Wesenheit template (Fig. 4) unifies variables of the instability strip to mitigate uncertainties tied to establishing a distance scale based on Cepheids, RR Lyrae, or δ Sct variables individually. Anchoring the distance scale via the universal Wesenheit template (Fig. 4) mobilizes the statistical weight of the entire variable star demographic to ensure a precise distance determination. Moreover, the universal Wesenheit template may be calibrated directly via parallaxes and apparent magnitudes, mitigating the propagation of uncertainties tied to extinction corrections. F. Benedict and coauthors are presently acquiring HST parallaxes for additional population II variables which shall bolster the template (Feast 2008). Further calibration could likewise ensue via vari-

ables in clusters with distances secured by dynamical means or eclipsing binaries (Cluster AgeS Experiment, Pietrukowicz & Kaluzny 2004; Guinan & Engle 2006; Kaluzny et al. 2007), and variables in the Galactic bulge that are tied to a precise geometric-based distance (Kubiak & Udalski 2003; Eisenhauer et al. 2005; Reid et al. 2009, supported by observations from the upcoming VVV survey; Minniti et al. 2010).

Lastly, Majaess et al. (2010) plotted the universal Wesenheit template (Fig. 4) as a function of the fundamentalized period to highlight the *first-order* VI period-magnitude continuity between RR Lyrae and Type II Cepheid variables (Matsunaga et al. 2006; Majaess 2009, see also Marconi & Di Criscienzo 2007 and references therein). The Wesenheit template presented here as Fig. 4 is plotted as a function of the dominant period, so pulsation modes may be inferred directly from the diagram.

3.3. PULSATION MODE

Wesenheit ridges in Fig. 4 that define δ Scutis pulsating in the fundamental, first, second, and third overtone

³<http://nedwww.ipac.caltech.edu/level5/NED1D/intro.html>

⁴<http://nedwww.ipac.caltech.edu/Library/Distances/>

Table 3: A Comparison of δ Sct Pulsation Modes

Star	Cluster	$n(W_{VI})$	n	Source
EX Cnc	M67	>3	3	Z05
EW Cnc	M67	1 or 0	0	Z05
HD 23156	Pleiades	1	0	F06
HD 23194	Pleiades	>3	4	F06
HD 23567	Pleiades	1 or 2	0	F06
HD 23607	Pleiades	1	0	F06
HD 23628	Pleiades	1	0	F06
HD 23643	Pleiades	1 or 0	0	F06
HD 73175	Praesepe	>3	3	P98
HD 73450	Praesepe	1	1	P98
HD 73575	Praesepe	≥ 3	3/?	P98
HD 73576	Praesepe	≥ 3	3	P98
HD 73763	Praesepe	>3	3/?	P98
HD 74028	Praesepe	≥ 3	3	P98

Notes: pulsation modes (primary signal, order n) inferred for M67, Pleiades, and Praesepe δ Scutis from the Wesenheit template (Fig. 4, $n(W_{VI})$) and sources in the literature (n). Sources are Zhang et al. (2005, Z05), Fox Machado et al. (2006, F06), and Pena et al. (1998, P98).

were constructed from data presented in Poleski et al. (2010, LMC) and Majaess et al. (2010, Galactic). LMC and Galactic δ Scutis pulsating in the overtone exhibit brighter VI Wesenheit magnitudes (W_{VI}) than their fundamental mode counterparts at a given period (Fig. 4, or bottom panel of Fig. 4 in Poleski et al. 2010). However, a clear separation was less evident in Garg et al. (2010) shorter-wavelength (VR) observations of LMC δ Scutis (their Fig. 3), thereby motivating those authors to favour an alternate conclusion. The present research relies on VI observations of δ Scutis.

Estimates of the pulsation modes (order, n) for the cluster δ Scutis were inferred from the Wesenheit template (Fig. 4) and are summarized in Table 4. Pulsation modes established from Wesenheit and seismological analyses for δ Scutis in the Pleiades, Praesepe, and M67 are comparable within the mutually expected (albeit large) uncertainties ($\pm n$) (Table 3). The methods identify high and low order pulsators in consistent fashion (e.g., HD23194 and HD73450, Table 3). Most small-amplitude cluster δ Scutis lie on Wesenheit loci characterizing $n \geq 1$ pulsators (non-fundamental mode, Fig. 4 and Table 4), and a sizable fraction are associated with $n = 1$ (Table 4). The results are consistent with Poleski et al. (2010) findings and past predictions (Breger 2000; McNamara et al. 2007, and references therein).

A primary source of uncertainty associated with the analysis rests with the pulsation periods adopted. Periods for the cluster δ Scutis were taken from Rodríguez et al. (2000), the GCVS (Samus et al. 2009a),

and the AAVSO’s VSX archive⁵ (Watson, Henden & Price 2010). In several instances discrepant periods are cited and newer estimates were favoured (SAO 38754, Li 2005). Efforts to extract the primary pulsation period (high SNR) for mmag δ Scutis in α Persei from ARO observations were unsuccessful, likely owing to increased humidity tied to summertime observations in Nova Scotia. That underscores the challenge such mmag pulsators present to low altitude observatories near sea-level. An additional source of uncertainty arises from a companion’s influence on the observed Wesenheit magnitudes. The pulsation mode assigned to HD 28052, which is a spectroscopic binary and bright X-ray source, should therefore be interpreted cautiously (Table 4). A star’s non-radial and multi-mode pulsation, and rotation/inclination along the line of sight likewise complicate a determination of n solely from the pulsation period and Wesenheit magnitude. Constraints established by Wesenheit analyses are admittedly limited by comparison to those inferred from uninterrupted space-based μ mag time-series photometry (MOST, COROT, Kepler), yet the Wesenheit approach is a viable first-order tool that can be applied promptly to δ Scutis in any field and concurrently with other methods.

3.4. δ SCT DISTANCE TO NGC1817

A potential role for mmag δ Scutis as distance indicators for intermediate-age open clusters is now explored using the aforementioned framework.

Arentoft et al. (2005) observations of NGC 1817 indicated that the open cluster hosts a statistically desirable sample of 11 δ Scutis. Balaguer-Núñez et al. (2004) proper motions implied that five of those stars are not cluster members (V1, V6, V8, V10, V12, see Arentoft et al. 2005). Yet Arentoft et al. (2005) concluded that 11 variables (V1→V12, excluding V10) exhibit positions in V vs. $B - V$ and $b - y$ colour-magnitude diagrams consistent with δ Sct pulsation and cluster membership. A *preliminary* V vs. $V - I$ colour-magnitude diagram for NGC 1817 (Fig. 5) confirms that most variables display positions consistent with membership (except V10). The VI data were obtained from the ARO and processed using ARAP⁶ (Lane 2007) and DAOPHOT⁷ (Stetson 1987). The ARO features an SBIG ST8XME CCD mounted upon a 35-cm telescope located near Stillwater Lake, Nova Scotia, Canada. The ARO is a remotely operated robotic observatory (Lane 2007). A description of the ARO observations for NGC 7062, including an analysis using VaST (Sokolovsky & Lebedev 2005), shall be provided in a subsequent study.

The VI Wesenheit diagram compiled for the δ Scutis

⁵<http://www.aavso.org/vsx/>

⁶<http://www.davelane.ca/aro/arap.html>

⁷IRAF contains DAOPHOT, however a standalone newer edition can be obtained from Peter.Stetson@nrc-cnrc.gc.ca

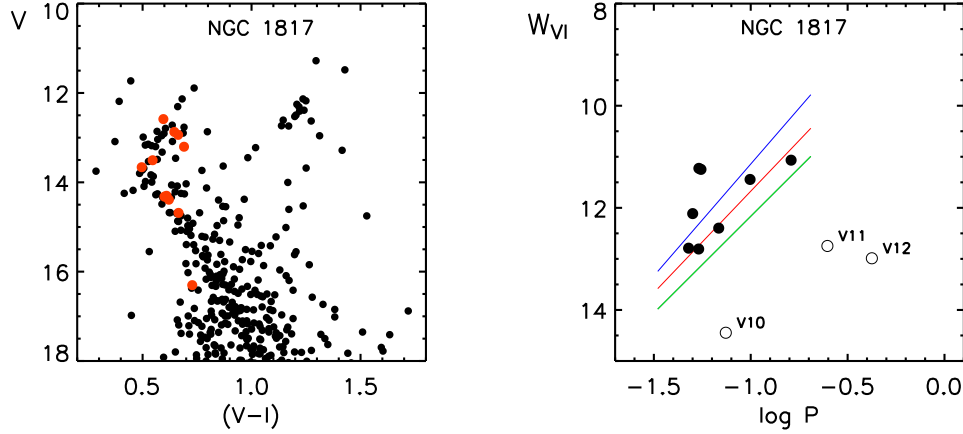


Fig. 5.— Left, a *preliminary* VI colour-magnitude diagram for the open cluster NGC 1817 compiled from ARO observations. A subsample of Arentoft et al. 2005 list of δ Scutis are highlighted by red dots. Right, the δ Scutis are featured in a Wesenheit diagram where green, red, and blue ridges correspond to $n = 0, 1, 3$ pulsators accordingly (right to left). The offset from the absolute Wesenheit magnitudes (Fig. 4) yields $d \simeq 1.7$ kpc, assuming the variables define the $n \geq 1$ boundary (see §3.3).

(Fig. 5) implies that V10, V11, and V12 either exhibit spurious data, are not *bona fide* δ Scutis, or are not cluster members. V10 is too faint, as corroborated by its position in the colour-magnitude diagram (Fig. 5). The variability detected in V11 is marred by low signal to noise and other complications (Arentoft et al. 2005). V12 is likewise too faint (W_{VI}) and features a period beyond that typically expected for δ Sct variables (Percy 2007). An advantage to applying the Wesenheit technique is that high and low-order pulsators may be identified. V1, V2, and V6 are likely pulsating at higher orders if the stars are members (Fig. 5). V3, V4, V7, V8, and V9 are tightly clustered and may define the $n \geq 1$ boundary (Fig. 5, see §3.3). The resulting distance to NGC 1817 is $d \simeq 1.7$ kpc, assuming the aforementioned mode distribution. The δ Sct distance to NGC 1817 agrees with estimates established for the cluster by other means (Arentoft et al. 2005, see references therein). However, employing mmag δ Scutis as distance indicators for open clusters is complicated by the need for independently confirmed periods, and *a priori* knowledge of the pulsation modes or the adoption of a mode distribution ($n \geq 1$) given sizable statistics (see §3.3). Establishing the distance to NGC 1817 or the Praesepe under the latter caveat may yield a pertinent result, yet the ensuing distance to α Persei would be in error owing to small statistics. α Persei certainly features more than 3 δ Scutis, however a detection bias emerges since nearby clusters exhibit large angular diameters which exceed the field of view of most CCDs. Continued research is needed.

4. SUMMARY AND FUTURE RESEARCH

This research aimed to outline and evaluate a VI Wesenheit framework for investigating cluster δ Scutis, an analysis which relied on securing absolute Wesenheit magnitudes from precise open cluster distances. JHK_s ZAMS and colour-colour relations were derived from unreddened stars near the Sun with precise Hipparcos parallaxes and were applied to infer parameters for several benchmark star clusters which host δ Scutis (Fig. 1, Table 1). That analysis yielded constraints on the absolute Wesenheit magnitudes ($W_{VI,0}$), evolutionary status, and pulsation modes (order, n) for the cluster δ Scutis (Figs. 2, 4, Tables 3, 4). VI photometry for the variables were tabulated to facilitate further research (Table 4), and include new data acquired via the AAVSO's robotic telescopes (Table 2).

The JHK_s established cluster distances are bolstered by the relative insensitivity of $J - K_s$ photometry to variations in $[\text{Fe}/\text{H}]$ and age over the baseline examined (§2.1, Table 1, Fig. 3). The deep JHK_s photometry extends into the low mass regime ($\simeq 0.4M_\odot$) and indicates that the clusters feature a common ZAMS in the infrared, and that $J - K_s$ remains constant with increasing magnitude ($M_J \gtrsim 6$) for low mass M-type dwarfs whereas $J - H$ exhibits an inversion (§2.1, Figs. 1, 2). The trends ensure precise ($\leq 5\%$) JHK_s ZAMS fits by providing distinct anchor points in colour-magnitude and colour-colour diagrams (Figs. 1, 2). JHK_s distances for 7 of 9 clusters within 250 pc agree with van Leeuwen (2009a) revised Hipparcos estimates (Table 1). However, the JHK_s distance to the Pleiades supports the HST estimate rather than that derived from Hipparcos data (Table 1). van Leeuwen (2009a,b) argues in favour of the revised Hipparcos distances to open clusters and

the reader is referred to that comprehensive study. Yet the distance scale can (presently) rely on a suite of clusters that are independent of the Pleiades. Models should be calibrated and evaluated using those nearby clusters where consensus exists regarding the distances (Table 1).

The general agreement between the JHK_s distances derived here and van Leeuwen (2009a) Hipparcos estimates is noteworthy (Table 1). The $\sim 10 - 20\%$ offset in distance for the discrepant cases (Pleiades & Blanco 1) is not atypical for studies of open clusters (Fig. 2 in Paunzen & Netopil 2006, see also Dias et al. 2002; Mermilliod & Paunzen 2003). Several clusters feature distance estimates spanning nearly a factor of two, such as NGC 2453 (Majaess et al. 2007, their Table 4), ESO 096-SC04, Collinder 419, Shorlin 1, and Berkeley 44 (Turner 2010b,c). The universal VI Wesenheit template could be applied to cluster δ Scuti so to isolate viable distance solutions, provided certain criteria are satisfied (§3.4, e.g., sizable statistics). A Wesenheit analysis (VI) is a viable means for establishing pertinent constraints on a target population of δ Sct variables, particularly in tandem with other methods (Figs. 2, 4, 5, Tables 3, 4).

ACKNOWLEDGEMENTS

DJM is grateful to the following individuals and consortia whose efforts and surveys were the foundation of this study: 2MASS (R. Cutri, M. Skrutskie, S. Nikolaev), OGLE (I. Soszyński, R. Poleski, M. Kubiak, A. Udalski), F. van Leeuwen, F. Benedict, Z. Li, E. Michel, T. Arentoft, P. Stetson (DAOPHOT), B. Taylor, WebDA/GCPD (E. Paunzen, J.-C. Mermilliod), NOMAD (N. Zacharias), TASS (T. Droege, M. Sallman, M. Richmond), NED (I. Steer), PASTEL (C. Soubiran), Astrometry.net (Lang et al. 2010), Skiff (2010), CDS, AAVSO (M. Saladyga, A. Henden), arXiv, and NASA ADS. T. Krajci, J. Bedient, D. Welch, D. Starkey, A. Henden, and others kindly funded the AAVSO's BSM.

REFERENCES

Alonso, A., Arribas, S., & Martinez-Roger, C. 1996, *A&A*, 313, 873
Arentoft, T., Bouzid, M. Y., Sterken, C., Freyhammer, L. M., & Frandsen, S. 2005, *PASP*, 117, 601
Artigau, E., Bouchard, S., Doyon, R., & Lafrenière, D. 2009, *ApJ*, 701, 1534
Artigau, E., Lamontagne, R., Doyon, R., & Malo, L. 2010, *Proc. SPIE*, 7737,
Balaguer-Núñez, L., Jordi, C., Galadí-Enríquez, D., & Zhao, J. L. 2004, *A&A*, 426, 819
Benedict G. F. et al., 2002 (a), *AJ*, 123, 473
Benedict, G. F., et al. 2002 (b), *AJ*, 124, 1695
Benedict G. F. et al., 2007, *AJ*, 133, 1810
Bonatto, C., Bica, E., & Santos, J. F. C. 2008, *MNRAS*, 386, 324
Bono, G., & Marconi, M. 1999, *New Views of the Magellanic Clouds*, 190, 527
Bono, G. 2003, *Stellar Candles for the Extragalactic Distance Scale*, 635, 85
Bono, G., Caputo, F., Fiorentino, G., Marconi, M., & Musella, I. 2008, *ApJ*, 684, 102
Breger, M. 2000, *Delta Scuti and Related Stars*, 210, 3
Catelan, M. 2009, *Ap&SS*, 320, 261
Cutri, R. M., et al. 2003, *The IRSA 2MASS All-Sky Point Source Catalog*, NASA/IPAC Infrared Science Archive.

Dias, W. S., Alessi, B. S., Moitinho, A., & Lépine, J. R. D. 2002, *A&A*, 389, 871
Di Criscienzo, M., Marconi, M., & Caputo, F. 2004, *ApJ*, 612, 1092
Di Criscienzo, M., Caputo, F., Marconi, M., & Cassisi, S. 2007, *A&A*, 471, 893
Droege T. F., Richmond M. W., Sallman M. P., Creager R. P., 2006, *PASP*, 118, 1666
Eisenhauer, F., et al. 2005, *ApJ*, 628, 246
Feast, M. W. 2008, arXiv:0806.3019
Fox Machado, L., Pérez Hernández, F., Suárez, J. C., Michel, E., & Lebreton, Y. 2006, *A&A*, 446, 611
Freedman, W. L., & Madore, B. F. 2010, arXiv:1004.1856
Garg, A., et al. 2010, *AJ*, 140, 328
Guinan, E. F., & Engle, S. G. 2006, *Ap&SS*, 304, 5
Henden, A. A., & Kaitchuck, R. H. 1990, *Richmond, Va. : Willmann-Bell*, c1990.
Henden, A. A. 2002, *JAAVSO*, 31, 11
Henden, A. A., & Sallman, M. P. 2007, *The Future of Photometric, Spectrophotometric and Polarimetric Standardization*, 364, 139
Henden, A., & Munari, U. 2008, *Information Bulletin on Variable Stars*, 5822, 1
Herrnstein, J. R., et al. 1999, *Nature*, 400, 539
Joner, M. D., Taylor, B. J., Laney, C. D., & van Wyk, F. 2006, *AJ*, 132, 111
Kaluzny, J., Thompson, I. B., Rucinski, S. M., Pych, W., Stachowski, G., Krzeminski, W., & Burley, G. S. 2007, *AJ*, 134, 541
Kovács, G., & Jurcsik, J. 1997, *A&A*, 322, 218
Kovács, G., & Walker, A. R. 2001, *A&A*, 371, 579
Kubiak M., Udalski A., 2003, *Acta Astr.*, 53, 117
Landolt, A. U. 1983, *AJ*, 88, 439
Landolt, A. U. 1992, *AJ*, 104, 340
Lane D. J., 2007, 96th Spring Meeting of the AAVSO, <http://www.aavso.org/aavso/meetings/spring07present/Lane.ppt> (see also <http://www.davelane.ca/aro/>)
Lang, D., Hogg, D. W., Mierle, K., Blanton, M., & Roweis, S. 2010, *AJ*, 139, 1782
Li, Z. P., & Michel, E. 1999, *A&A*, 344, L41
Li, Z. P. 2005, *AJ*, 130, 1890
Macri, L. M., Stanek, K. Z., Bersier, D., Greenhill, L. J., & Reid, M. J. 2006, *ApJ*, 652, 1133
Macri, L. M., & Riess, A. G. 2009, *American Institute of Physics Conference Series*, 1170, 23
Madore B. F., 1982, *ApJ*, 253, 575
Madore, B. F., & Freedman, W. L. 1991, *PASP*, 103, 933
Madore, B. F., & Steer, I. 2007, *NASA/IPAC Extragalactic Database Master List of Galaxy Distances* (<http://nedwww.ipac.caltech.edu/level5/NED1D/intro.html>)
Madore, B. F., & Freedman, W. L. 2009, *ApJ*, 696, 1498
Majaess, D. J., Turner, D. G., & Lane, D. J. 2007, *PASP*, 119, 1349
Majaess D. J., Turner D. G., Lane D. J., 2008, *MNRAS*, 390, 1539
Majaess, D. J., Turner, D. G., & Lane, D. J. 2009 (a), *MNRAS*, 398, 263
Majaess, D., Turner, D., & Lane, D. 2009 (b), *Acta Astronomica*, 59, 403
Majaess, D. J. 2009, arXiv:0912.2928
Majaess, D. 2010 (a), *Acta Astronomica*, 60, 55
Majaess, D. J. 2010 (b), *Acta Astronomica*, 60, 121
Majaess, D. J., Turner, D. G., Lane, D. J., Henden, A., & Krajci, T. 2010, arXiv:1007.2300
Marconi, M., & Di Criscienzo, M. 2007, *A&A*, 467, 223
Matsunaga, N., et al. 2006, *MNRAS*, 370, 1979
McNamara, D. H., Madsen, J. B., Barnes, J., & Ericksen, B. F. 2000, *PASP*, 112, 202
McNamara, D. H., Clementini, G., & Marconi, M. 2007, *AJ*, 133, 2752
Mendoza, E. E. 1967, *Boletín de los Observatorios Tonantzintla y Tacubaya*, 4, 149

Table 4: δ Scutis in Benchmark Open Clusters

Star	Cluster	CMD position (Fig. 2)	$n(W_{VI})$	VI Photometry
SAO 38754	α Persei	MS	1	TASS, S85
HD 20919	α Persei	MS,BR:	2 or 3	TASS
HD 21553	α Persei	MS	0	TASS
HD 23156	Pleiades	MS	1	Table 2
HD 23194	Pleiades	MS	>3	Table 2
HD 23567	Pleiades	MS	1 or 2	Table 2
HD 23607	Pleiades	MS	1	Table 2
HD 23628	Pleiades	MS,BR	1	Table 2
HD 23643	Pleiades	MS,BR	1 or 0	Table 2
HD 27397	Hyades	EV	1 or 2	T85
HD 27459	Hyades	EV	1	J06
HD 27628	Hyades	sat./EV:	1	J06
HD 28024	Hyades	sat./EV:	1 or 0	J06
HD 28052	Hyades	sat./EV:	0	J06
HD 28319	Hyades	sat./EV:	>3	J06
HD 30780	Hyades	sat.	>3	J06
HD 73175	Praesepe	MS/EV	>3	TASS, ME67
HD 73345	Praesepe	MS/EV	>3	TASS, ME67
HD 73450	Praesepe	MS	1	TASS, ME67
HD 73575	Praesepe	EV	≥ 3	TASS, ME67
HD 73576	Praesepe	MS/EV,BR	≥ 3	TASS, ME67
HD 73712	Praesepe	EV	1 or 2	TASS, ME67
HD 73729	Praesepe	MS/EV,BR	2 or 3	TASS, ME67
HD 73746	Praesepe	MS	1	TASS, ME67
HD 73763	Praesepe	MS/EV	>3	TASS, ME67
HD 73798	Praesepe	MS/EV	1	TASS, ME67
HD 73819	Praesepe	EV	0	TASS, ME67
HD 73890	Praesepe	MS/EV,BR	>3	TASS, ME67
HD 74028	Praesepe	MS/EV	≥ 3	TASS, ME67
HD 74050	Praesepe	MS/EV	3	TASS, ME67
EX Cnc	M67	BS	>3	Table 2
EW Cnc	M67	BS	1 or 0	Table 2

Notes: δ Sct cluster list compiled primarily from Li & Michel (1999) and references therein. The identifiers are as follows: stars occupying the blue straggler region (BS), binary / rapid rotator sequence (BR), evolved region (EV), and main-sequence (MS) of the colour-magnitude diagram (Fig. 2); Pulsation modes (primary signal, order n) inferred for the δ Scutis from the VI Wesenheit template (Fig. 4). Hyades members may feature saturated (sat.) 2MASS photometry owing to their proximity (Table 1). There are concerns regarding the photometric zero-point for bright δ Scutis sampled in the all-sky surveys (Henden & Sallman 2007). References for the photometry are Mendoza (1967, ME67), Taylor & Joner (1985, T85), Stauffer et al. (1985, S85), and Joner et al. (2006, J06).

- Mermilliod, J.-C. 1991, Homogeneous Means in the UBV System, R. M., Wheelock, S. L., Gizis, J. E., & Howard, E. M. 2000, AJ, 120, 3340
- <http://vizier.u-strasbg.fr/viz-bin/VizieR?-source=II/168> Opolski A., 1983, IBVS, 2425, 1
- Mermilliod, J.-C., Turon, C., Robichon, N., Arenou, F., & Opolski, A. 1988, Acta Astronomica, 38, 375
- Lebreton, Y. 1997, Hipparcos - Venice '97, 402, 643 Percy, J. R. 2007, Understanding variable stars / Cambridge University Press
- Mermilliod, J.-C., & Paunzen, E. 2003, A&A, 410, 511 Paunzen, E., & Netopil, M. 2006, MNRAS, 371, 1641
- Minniti, D., et al. 2010, New Astronomy, 15, 433 Paunzen, E., Heiter, U., Netopil, M., & Soubiran, C. 2010, A&A, 517, A32
- Mochejska, B. J., Macri, L. M., Sasselov, D. D., & Stanek, K. Z. 2001, arXiv:astro-ph/0103440
- Nikolaev, S., Weinberg, M. D., Skrutskie, M. F., Cutri, Pena, J. H., et al. 1998, A&AS, 129, 9

- Percival, S. M., Salaris, M., & Groenewegen, M. A. T. 2005, *A&A*, 429, 887
- Perryman, M. A. C., & ESA 1997, ESA Special Publication, 1200
- Petersen, J. O., & Høg, E. 1998, *A&A*, 331, 989
- Pietrukowicz, P., & Kaluzny, J. 2004, *Acta Astronomica*, 54, 19
- Pietrzyński, G., Gieren, W., Udalski, A., Bresolin, F., Kudritzki, R.-P., Soszyński, I., Szymański, M., & Kubiak, M. 2004, *AJ*, 128, 2815
- Poleski, R., et al. 2010, *Acta Astronomica*, 60, 1
- Reid, M. J., Menten, K. M., Zheng, X. W., Brunthaler, A., & Xu, Y. 2009, *ApJ*, 705, 1548
- Robichon, N., Arenou, F., Mermilliod, J.-C., & Turon, C. 1999 (a), *A&A*, 345, 471
- Robichon, N., Arenou, F., Lebreton, Y., Turon, C., & Mermilliod, J. C. 1999 (b), *Harmonizing Cosmic Distance Scales in a Post-HIPPARCOS Era*, 167, 72
- Rodríguez, E., López-González, M. J., & López de Coca, P. 2000, *A&AS*, 144, 469
- Romaniello, M., et al. 2008, *A&A*, 488, 731
- Samus, N. N., Durlevich, O. V., & et al. 2009, *VizieR Online Data Catalog*, 1, 2025
- Sarajedini, A., Dotter, A., & Kirkpatrick, A. 2009, *ApJ*, 698, 1872
- Skrutskie, M. F., et al. 2006, *AJ*, 131, 1163
- Skiff, B. 2010, *Catalogue of Stellar Spectral Classifications*, <http://vizier.u-strasbg.fr/viz-bin/VizieR?-source=B/mk>
- Smith, H. A. 2004, *RR Lyrae Stars*, by Horace A. Smith, pp. 166. ISBN 0521548179. Cambridge, UK: Cambridge University Press, September 2004
- Smith, M. C., Woźniak, P., Mao, S., & Sumi, T. 2007, *MNRAS*, 380, 805
- Soderblom, D. R., Nelan, E., Benedict, G. F., McArthur, B., Ramirez, I., Spiesman, W., & Jones, B. F. 2005, *AJ*, 129, 1616
- Soderblom, D. R., Laskar, T., Valenti, J. A., Stauffer, J. R., & Rebull, L. M. 2009, *AJ*, 138, 1292
- Sokolovsky, K., & Lebedev, A. 2005, 12th Young Scientists' Conference on Astronomy and Space Physics, 79
- Soszyński, I., et al. 2002, *Acta Astronomica*, 52, 369
- Soszyński, I., et al. 2003, *Acta Astronomica*, 53, 93
- Soszyński, I., et al. 2008, *Acta Astronomica*, 58, 293
- Soszyński, I., et al. 2008 (b), *Acta Astronomica*, 58, 163
- Soszyński, I., et al. 2009, *Acta Astronomica*, 59, 1
- Soubiran, C., Le Campion, J.-F., Cayrel de Strobel, G., & Caillo, A. 2010, *A&A*, 515, A111
- Stanek, K. Z., & Udalski, A. 1999, *arXiv:astro-ph/9909346*
- Stauffer, J. R., Hartmann, L. W., Burnham, J. N., & Jones, B. F. 1985, *ApJ*, 289, 247
- Stauffer, J. R., Jones, B. F., Backman, D., Hartmann, L. W., Barrado y Navascués, D., Pinsonneault, M. H., Terndrup, D. M., & Muench, A. A. 2003, *AJ*, 126, 833
- Steer, I. & Madore, B. F. 2010, *NED-D: A Master List of Redshift-Independent Extragalactic Distances* (<http://nedwww.ipac.caltech.edu/Library/Distances/>)
- Stetson, P. B. 1987, *PASP*, 99, 191
- Straizys, V., & Laugalys, V. 2009, *Baltic Astronomy*, 18, 141
- Taylor, B. J., & Joner, M. D. 1985, *AJ*, 90, 479
- Taylor, B. J. 2008, *AJ*, 136, 1388
- Templeton, M. R. 2009, *Astronomical Society of the Pacific Conference Series*, 412, 187
- Turner, D. G. 1979, *PASP*, 91, 642
- Turner, D. G., Majaess, D. J., Lane, D. J., Szabados, L., Kovtyukh, V. V., Usenko, I. A., & Berdnikov, L. N. 2009, *American Institute of Physics Conference Series*, 1170, 108
- Turner, D. G. 2010 (a), *Ap&SS*, 326, 219
- Turner, D. G. 2011 (b), *arXiv:1102.0347*
- Turner, D. G. 2010 (c), *submitted*.
- Udalski A. et al., 1999, *Acta Astr.*, 49, 223
- Udalski, A., Wyrzykowski, L., Pietrzynski, G., Szweczyk, O., Szymanski, M., Kubiak, M., Soszyński, I., & Zebrun, K. 2001, *Acta Astronomica*, 51, 221
- Udalski, A. 2009, *Astronomical Society of the Pacific Conference Series*, 403, 110
- van Altena, W. F., et al. 1997, *ApJ*, 486, L123
- van Leeuwen, F. 1999, *A&A*, 341, L71
- van Leeuwen, F. 2007, *A&A*, 474, 653
- van Leeuwen, F. 2009 (a), *A&A*, 497, 209
- van Leeuwen, F. 2009 (b), *A&A*, 500, 505
- Vilardell, F., Jordi, C., & Ribas, I. 2007, *A&A*, 473, 847
- Watson, C., Henden, A. A., & Price, A. 2010, *VizieR Online Data Catalog*, 1, 2027
- Zacharias, N., Monet, D. G., Levine, S. E., Urban, S. E., Gaume, R., & Wycoff, G. L. 2004, *Bulletin of the American Astronomical Society*, 36, 1418
- Zhang, X.-B., Zhang, R.-X., & Li, Z.-P. 2005, *Chinese J. Astron. Astrophys.*, 5, 579